Title	Cubitus varus deformity following paediatric supracondylar humeral fracture remodelling predominantly in the sagittal direction: A three-dimensional analysis of eighty-six cases
Author(s)	Miyake, Tasuku; Miyamura, Satoshi; Miki, Ryo et al.
Citation	International Orthopaedics. 2024, 48, p. 2091-2099
Version Type	VoR
URL	https://hdl.handle.net/11094/97116
rights	This article is licensed under a Creative Commons Attribution 4.0 International License.
Note	

ORIGINAL PAPER

Cubitus varus deformity following paediatric supracondylar humeral fracture remodelling predominantly in the sagittal direction: A three-dimensional analysis of eighty-six cases

Tasuku Miyake[1] · Satoshi Miyamura[1] · Ryo Miki[2] · Ryoya Shiode[1] · Toru Iwahashi[1] · Arisa Kazui[1] · Natsuki Yamamoto[1] · Hiroyuki Tanaka[1,3] · Seiji Okada[1] · Tsuyoshi Murase[1,4] · Kunihiro Oka[1,5]

Abstract

Purpose Three-dimensional (3D) capacity for remodelling in cubitus varus deformity (CVD) after paediatric supracondylar humeral fractures (PSHFs) remains unelucidated. This study investigated remodelling patterns after PSHFs by examining 3D deformity distribution over time after injury.

Methods Computed tomography (CT) data of 86 patients with CVD after PSHFs were analysed. The 3D deformity angles in the sagittal, coronal, and axial directions were assessed and correlated with the duration between the age at injury and CT evaluation. For the subgroup analysis, we performed the same correlation analysis in a younger (<8 years old) and an older group (≥ 8 years old); we categorized the duration into early (<2 years), middle (≥ 2 to <5 years), and late periods (≥ 5 years) and compared the deformity angles of each direction among the three groups.

Results Sagittal deformity showed a moderate correlation with the duration of deformity ($r = -0.54$; $P < 0.001$), while coronal and axial deformities showed a negligible correlation. Sagittal deformity showed moderate correlations with the duration in the younger group ($r = -0.62$; $P < 0.001$) and weak correlations in the older group ($r = -0.37$; $P = 0.091$). In the sagittal direction, the deformity angle in the early period was significantly larger than those in the mid and late periods ($P < 0.001$). However, there were no significant differences among the three groups in the coronal and axial directions.

Conclusion Sagittal deformities in CVDs are capable of remodelling, especially in the early period and at a younger age, whereas coronal and axial deformities are less likely to undergo remodelling.

Keywords Cubitus varus deformity · Three-dimensional analysis · Remodelling · Complication after supracondylar fracture · Elbow

Introduction

Owing to inadequate treatment, paediatric supracondylar humeral fractures (PSHFs) often heal with deformities, most notably, cubitus varus deformity (CVD), in 10%–57% of cases [1–3]. The residual combined deformity comprises varus, extension, and rotation [3, 4], with unacceptable cosmetic defects that also induce functional effects, such as restricted motion at the elbow joint, recurrent fractures of the lateral humeral condyle [5], posterolateral rotatory instability [6], late ulnar nerve neuropathy [7, 8], and osteoarthritis (OA) [9, 10].

Nonetheless, fractures in children have a good capacity for remodelling. Although remodelling of sagittal angulation generally occurs [11–13], remodelling of the coronal and rotational malunion is not expected [12]. However, some

✉ Kunihiro Oka
oka-kunihiro@ort.med.osaka-u.ac.jp

1 Department of Orthopedic Surgery, Osaka University Graduate School of Medicine, Suita, Japan

2 Miki Orthopedic Surgery & Internal Medicine, Minoh, Japan

3 Department of Sports Medical Science, Osaka University Graduate School of Medicine, Suita, Japan

4 Department of Orthopedic Surgery, Bell Land General Hospital, Sakai, Japan

5 Department of Orthopedic Biomaterial Science, Osaka University Graduate School of Medicine, Suita, Japan

sceptical reports exist regarding the capacity for remodelling in the sagittal direction after PSHFs [14, 15].

Most reports on remodelling relied on a two-dimensional analysis using conventional radiographic measurements [11, 12, 16–18], which when compared with three-dimensional (3D) evaluation using computed tomography (CT), can generate an error of 10° or more in a CVD [3]. Furthermore, evaluating the residual rotational deformity on anteroposterior and lateral radiographs is challenging [3, 19, 20]. Although CVD remodelling should be evaluated three-dimensionally with CT, the 3D capacity of remodelling is unelucidated.

We hypothesized that CVDs would exhibit a unique remodelling pattern. We aimed to investigate the remodelling patterns following PSHFs by examining the distribution of 3D deformities over time after injury.

Materials and methods

Study Design

Ninety-two consecutive patients with CVD, who visited our institution between September 2005 and December 2022, underwent CT scanning of both elbows for an evaluation of the deformity or a preoperative simulation. This study was approved by our institutional review board. The requirement for written informed consent was waived because of the retrospective nature of the study.

The inclusion criterion was the presence of a CVD compared to the unaffected side, resulting from the malunion of a supracondylar fracture of the distal humerus. Six patients were excluded: four with elbow OA, one with bilateral deformities, and one with a congenital deformity. The remaining 86 patients (71 males, 15 females) were enrolled (Table 1). For remodelling evaluation, we calculated the age as 20 years if the patient was ≥20 years old at the time of CT evaluation because fracture remodelling is not expected after 20 years of age [21]. In the 12 patients aged ≥20 years,

Table 1 Characteristics of the study cohort

	Patients (n = 86)
Sex	71 males, 15 females
Affected side	Right, 43; Left, 43
Age at injury (years)	5.7 years (±2.6 years, 1–12)
Age at time of CT Scan (years)	11.4 years (±4.7 years, 4–20)
Duration of deformity (years)	5.8 years (±4.4 years, 0–17)
Initial treatment	Casting; 40 (47%)
	Pinning; 31 (36%)
	Unknown; 15 (17%)

CT, computed tomography

we confirmed on the plain radiographs that the epiphyseal line was closed.

Image Acquisition and 3D Bone Model Reconstruction

We used a helical-type CT scanner (LightSpeed Ultra 16 or 64; GE Healthcare, Waukesha, Wisconsin) with a low radiation-dose technique (slice thickness, 1.25 mm; pixel size, 0.75–0.85 mm; scan time, 0.5 s; scan pitch, 0.562:1; tube current, 20–150 mA and tube voltage, 120 kV) [3, 10, 22] to evaluate the 3D deformity. With the patient in the prone position, both the upper limbs were scanned with the shoulder at full elevation, the elbow at full extension, and the forearm maintained in supination. The digital data were saved and computer analysed. We created 3D surface models of the bilateral humerus, radius, and ulna from the digital data by semiautomatically segmenting individual osseous regions using a global threshold algorithm, with a threshold of 250 Hounsfield units (HU) [23] using MvIndex/Bone-Simulator image processing software (Teijin Nakashima Medical, Okayama, Japan).

Quantification of Deformity

To quantify deformities of the distal humerus, we used a modified orthogonal reference system originally advocated by the International Society of Biomechanics [24]. The origin was defined as the intersection of the humeral inertia axis (Y-axis) and the proximal end of the humeral head, and was indicated as distal (+) or proximal (-). The Z-axis was defined as the line connecting the origin and the parallel line connecting the lateral and medial epicondyle tips of the humerus that indicated the lateral (+) or medial (-) direction. The X-axis was defined as the line perpendicular to the YZ plane and indicated the posterior (+) or anterior (-) direction (Fig. 1).

To evaluate the 3D humerus deformity using a surface-based registration technique [25, 26], the affected humerus was compared with a mirror image of the contralateral normal humerus (Fig. 2). The 3D varus, extension, and internal rotation deformities were quantified by superimposing the proximal parts of the affected humerus onto those of the mirror image of the normal humerus and calculating the rotation angles of the distal parts, according to previous studies that used the Euler angle method [3, 10]. In this study, we calculated the absolute values of the deformity angles in the coronal, sagittal, and axial directions relative to those in the contralateral normal humerus to investigate the remodelling. In our cohort, 43 (50%), 19 (22%), 14 (16%), and ten (12%) participants had coronal–axial, triplane, coronal, and coronal–sagittal direction deformities, respectively; a deformity > 5° was considered significant [27, 28].

Fig. 1 Orthogonal coordinates of distal humerus. The coordinate system was a modified version of the International Society of Biomechanics reference system. The origin is the intersection of the humeral inertia axis (y-axis) and the proximal end of the humeral head. Z, Line connecting the origin and the parallel line connecting the lateral and medial epicondyle tips of the humerus; X, line perpendicular to the YZ plane
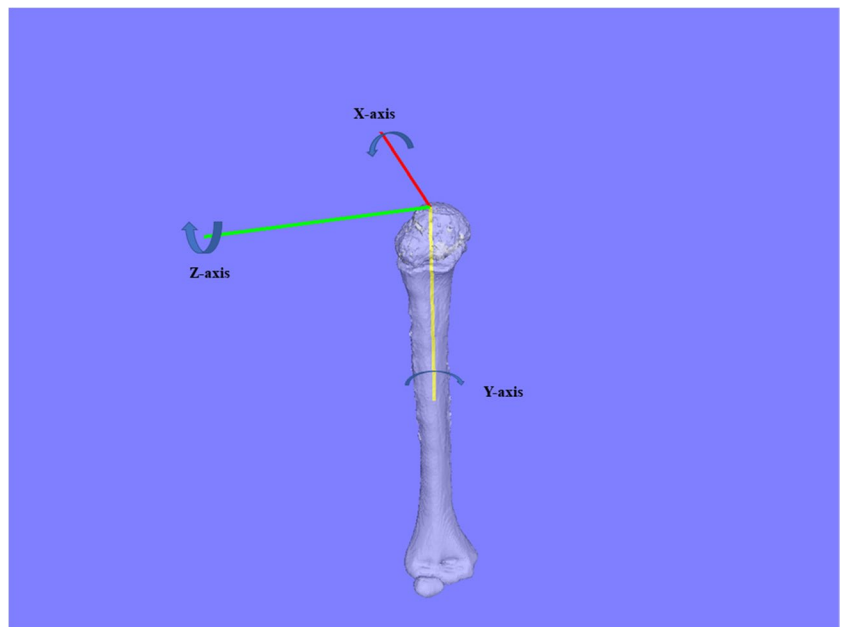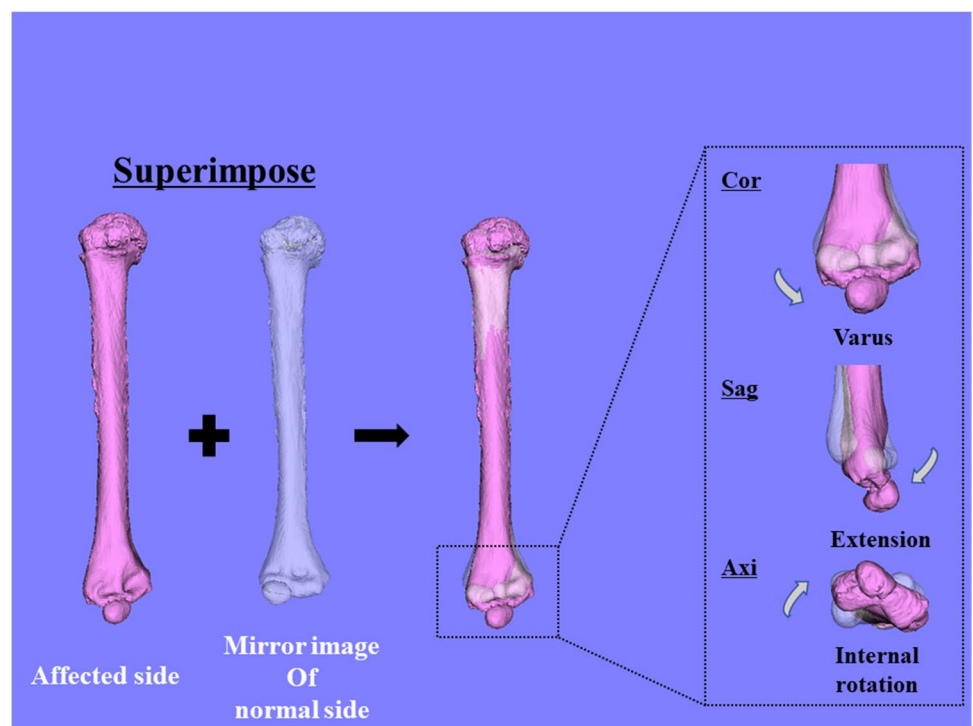
Fig. 2 Three-dimensional (3D) deformity of the distal humerus The proximal site of the affected humerus is superimposed on a mirror image of the contralateral normal humerus. Next, the 3D deformity of the distal site was quantified in three directions: varus (coronal direction), extension (sagittal direction), and rotation (axial direction)

Statistical analysis

All statistical analyses were performed using GraphPad Prism version 9.0 (San Diego, CA, USA); the significance level was set at a P-value < 0.05.

In general, supracondylar fractures of the humerus occur predominantly at four to seven years of age [16, 29], with a male-to-female ratio of 3:1 [30]. Only a varus deformity is seen in 20% of patients, whereas the remaining 80% have a combined deformity [3]. In the current cohort, the mean age at injury was 5.7 years, with a male-to-female ratio of 4.7:1; 14 cases (16%) showed only varus deformity. Therefore, we performed a correlation analysis to evaluate the trend in deformities with the assumption, based on previous reports, that the study population was a generalized population. This study did not follow changes in each patient over

time, but instead made fixed-point observations within the population to examine correlations. Spearman's correlation coefficients were determined between the 3-D deformity angle in each direction (sagittal, coronal, and axial) and the duration of deformity and between the 3D deformity and age at injury. The strength of correlation was classified as negligible ($|r| < 0.2$), low ($|r| = 0.2–0.4$), moderate ($|r| = 0.4–0.7$), or high ($|r| > 0.7$).

Subsequently, to examine the timing of remodelling, we divided the patients into three groups based on the duration between ages at injury and CT evaluation: an early-period (< 2 years), mid-period (≥ 2 to < 5 years), and a late-period (≥ 5 years) [31]. The 3D deformity angles were analysed using the Kruskal–Wallis nonparametric analysis followed by Dunn's multiple-comparison test to evaluate differences among the three periods in each direction.

Furthermore, using Spearman's correlation coefficient, we correlated the 3D deformity angles with the duration at injury in a younger group (< 8 years) and an older group (≥ 8 years) to investigate the impact of age at injury on remodelling. A threshold age of 8 years was determined, considering that children older than 8 years have minimal capacity to remodel sagittal plane malunion [11].

Power analysis performed to calculate the sample size necessary to detect the correlation (calculated with effect size $= 0.4$, alpha $= 0.05$, two-tailed, power $= 0.95$) indicated that a sample size of 71 participants was sufficient.

Results

In the study cohort, the right and left sides were affected in 43 patients each; the mean age at injury was 5.7 years (range, 1–12 years), and the mean age at the time of CT image acquisition was 11.4 years (range, 4–20 years). The mean interval between the original injury and image acquisition was 5.8 years (range, 0–17 years).

3D Humerus Deformity

The mean deformity angles in sagittal, coronal, and axial directions were $5.9° \pm 8.4°$ of extension, $16.8° \pm 5.6°$ of varus, and $11.8° \pm 9.4°$ of internal rotation, respectively.

Correlation Analysis Between 3D-deformity Angles and Duration of Deformity

There was a moderate negative correlation between the sagittal direction deformity and the duration of deformity ($r = -0.54$; $P < 0.001$). In contrast, coronal ($r = 0.17$; $P = 0.110$) and axial ($r = 0.01$; $P = 0.897$) deformities showed negligible correlations with the duration of deformity (Fig. 3).

Comparison of 3D-deformity Angles Among Early, Middle, and Late Periods in Each Deformity Direction

In the sagittal direction deformity, the deformity angle of the early-period ($15.1° \pm 12.6°$) was significantly higher than that of the middle ($3.1° \pm 2.3°$, $P < 0.001$) and late-periods ($2.6° \pm 2.5°$, $P < 0.001$); however, there was no significant difference between the deformity angles of the middle and late-periods ($P = 1.000$). In the coronal direction deformity, there was no significant difference among the deformity angles of early ($14.5° \pm 6.4°$), middle ($17.1° \pm 5.6°$), and late ($18.9° \pm 4.8°$) periods (early vs. middle, $P = 0.386$; early vs. late, $P = 0.173$; middle vs. late, $P = 1.000$). Similarly, in the axial direction deformity, there was no significant difference among the deformity angles of early ($11.8° \pm 10.2°$), middle ($11.1° \pm 8.8°$), and late ($12.4° \pm 9.8°$) periods (early vs. middle, $P = 1.000$; early vs. late, $P = 1.000$; and middle vs. late, $P = 1.000$); Fig. 4).

Correlation Analysis Between Deformity and Deformity Duration in the Younger and Older Groups

There was a moderate negative correlation between the sagittal direction deformity and the duration of deformity in the younger group ($r = -0.62$; $P < 0.001$), whereas there was a weak correlation between these in the older group ($r = -0.37$; $P = 0.091$). Coronal-direction deformities showed a weak correlation with duration in the younger group ($r = 0.23$; $P = 0.068$) and the older group ($r = 0.24$; $P = 0.283$). Axial-direction deformities showed a negligible correlation with duration in the younger group ($r = 0.10$; $P = 0.453$) and a low negative correlation in the older group ($r = -0.25$; $P = 0.255$; Fig. 5).

Discussion

We analysed the 3D capacity for remodelling after supracondylar humeral fracture (SHF) by investigating the distribution of deformity angles among 86 CVDs with varying periods since injury. Our results indicate that sagittal deformities are capable of remodelling, whereas coronal and axial deformities are less likely to undergo remodelling. A subgroup analysis revealed that the sagittal direction undergoes robust remodelling in the early period following injury, particularly in younger age groups.

Several studies have analysed CVD remodelling using conventional radiography, showing that deformities in the sagittal direction can be remodelled. Persiani et al. [15] analysed 62 children with extension-type SHFs with a mean follow-up of four years and three months. Guven et al. [32]
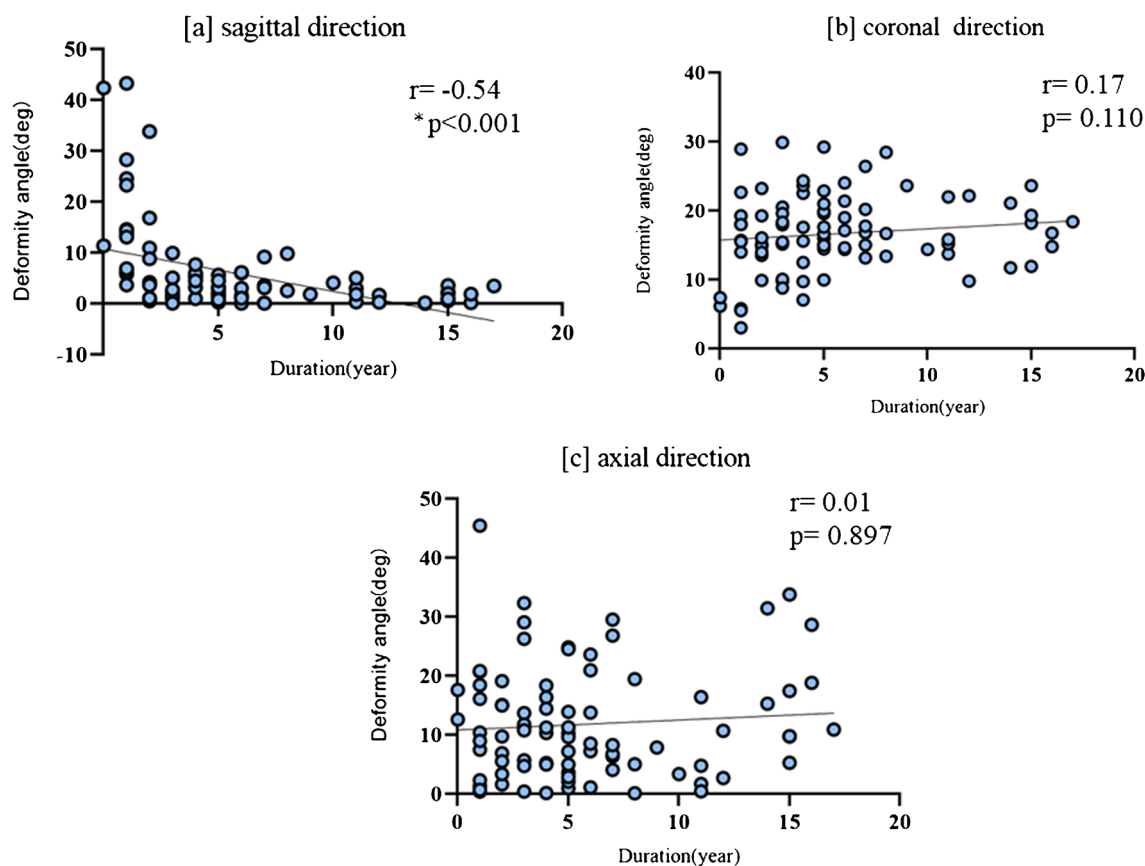
Fig. 3 The graph shows the correlation between 3D deformity angles and duration with deformity at each direction (**a**) Sagittal direction deformity; (**b**) Coronal direction deformity; and [c] Axial direction deformity. Only in the sagittal direction was a negative moderate correlation between them observed. SD, Three-dimensional

analysed data from 49 children with Gartland type 3 fractures with a mean follow-up of 22.4 years. Conventional radiographic measurements were obtained preoperatively and at the final follow-up to examine the remodelling in each direction; a greater capacity for remodelling was observed in the sagittal direction compared to that in the coronal direction. James et al. [11] reported 100% remodelling in the sagittal direction in 41 children under 5 years. However, many investigators proposed that deformity remodelling in the coronal direction is unlikely [16, 33–36], which has been consistently observed. Remodelling in the axial direction is as unlikely as in the coronal direction [37]; however, no studies have accurately evaluated remodelling in the axial direction using 3D images. The sagittal deformity angles showed a moderate negative correlation with the duration of the deformity when considering the time interval from injury. This indicates that sagittal deformities are capable of remodelling.

Fractures in children are typically remodelled according to Wolff's law [38]: new bone is laid down on the compressed or concave side of the long bone. Moreover, remodelling is more likely to occur spontaneously if the child is younger, if the fracture site is closer to the physis, or if there is a relative alignment of angulation in the normal plane of motion of the joint [37]. Our results showed that deformities in the sagittal direction were predominantly remodelled. Presumably, the direction of the sagittal deformity coincided with the direction of the flexion–extension motion of the elbow joint, which may have influenced the deformity remodelling in the sagittal direction. During elbow flexion, the flexor muscles overpower the extensor muscles, generating compressive forces on the flexor side of the fracture and traction forces on the opposite side. This results in active bone formation on the flexor side and bone resorption on the extensor side [37].

Although no previous report exists on the timing of remodelling after SHFs, distal radius fractures in children mainly remodel in the first year after injury and are less likely to remodel after ≥two 2 years [31, 39]. We found that sagittal deformity in the early period was significantly greater than that in the middle and late periods when classified into three groups, based on the duration between age at injury and CT evaluation. This indicates that the sagittal
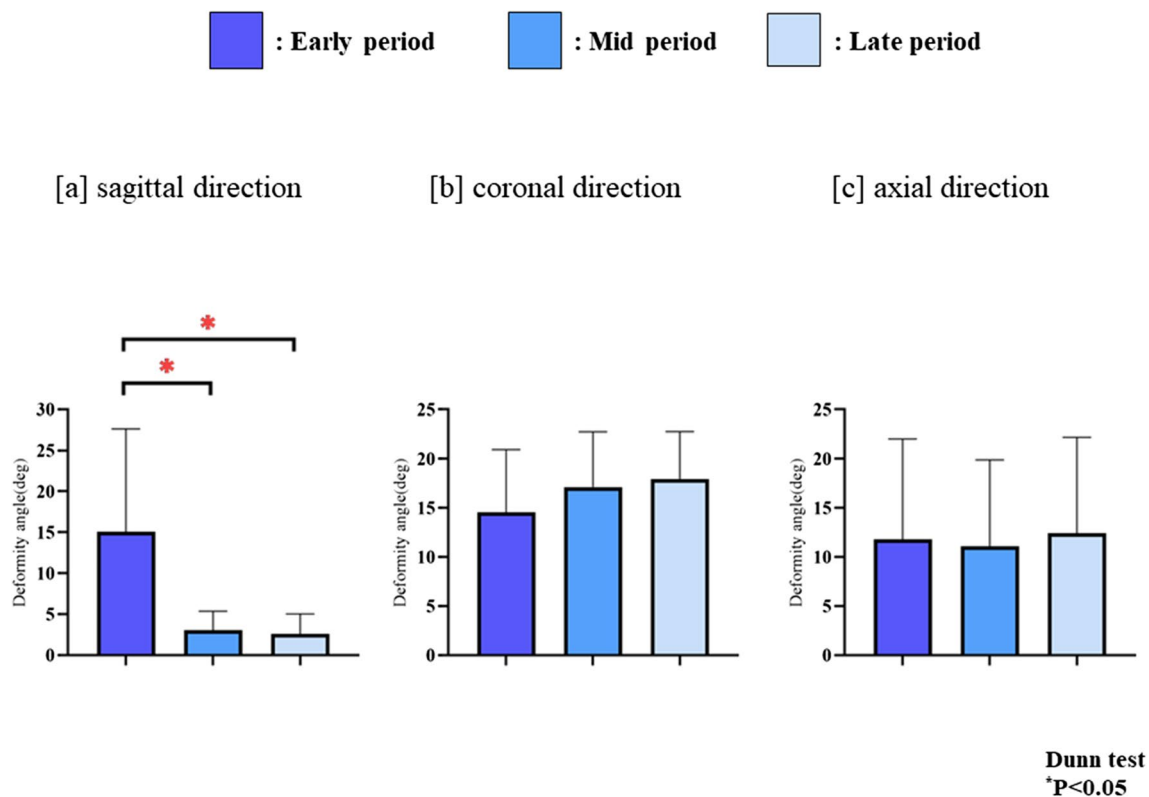
Fig. 4 Deformity angles In the sagittal direction deformity, the middle (n = 31) and late-stage (n = 33) groups showed significantly reduced deformity angles compared to those in the early-stage group (n = 22) (Kruskal–Wallis/Dunn's, $P < 0.05$)

deformity of the distal humerus was remodelled vigorously in the early period after SHFs, and.

in the younger group showed a moderate correlation with duration. In general, the younger the age at injury, the greater the ability to remodel. One possible explanation is that the periosteum and endosteum play important roles in bone remodelling, and these tissues are more active in the younger group, making remodelling more likely to occur [37]. Camus et al. [40] reported that children older than nine years may have a minimal capacity for remodelling, which supports the current findings that remodelling ability decreases with age with a threshold of eight years. In later life, posterolateral rotatory instability [6], late ulnar nerve neuropathy [7, 8], and osteoarthritis [9, 10] are known late complications of CVD, and these may be somehow related to the specific remodelling patterns identified in this study.

Collectively, residual deformities after SHFs can be remodelled in the sagittal direction, and sagittal remodelling is more likely to occur early after injury and at younger ages. These findings are useful for optimizing treatment strategies and evaluating the prognosis of fractures clinically. First, it is important to pay particular attention to the residual deformity in the coronal and axial directions at the initial treatment and during the follow-up period when treated conservatively or surgically. Second,

if these deformities remain cosmetically and functionally problematic, corrective osteotomy is necessary at any age to prevent these late complications because the deformities in the coronal and axial direction will not be remodelled. However, if the deformity in the sagittal direction is the predominant deformity, there is a possibility of remodelling, and the patients younger than 8 years should be followed up. Corrective osteotomy is then decided when there is functional impairment such as limited range of motion and remodelling is not expected.

The current study has some limitations. First, this study investigated the distribution of deformities in all age groups, and individual cases were not followed up. However, we believe that remodelling can be evaluated by investigating the distribution because we extracted data from the general population after SHFs. Second, patient information was limited to medical records and X-ray/CT images because this was a retrospective study.

In conclusion, with CVD following PSHF, there was a predominant correlation between sagittal deformity and duration. Sagittal deformities are capable of remodelling, whereas coronal and axial deformities are less likely to undergo remodelling.

We believe that our findings will improve the understanding of the remodelling potential of CVDs.
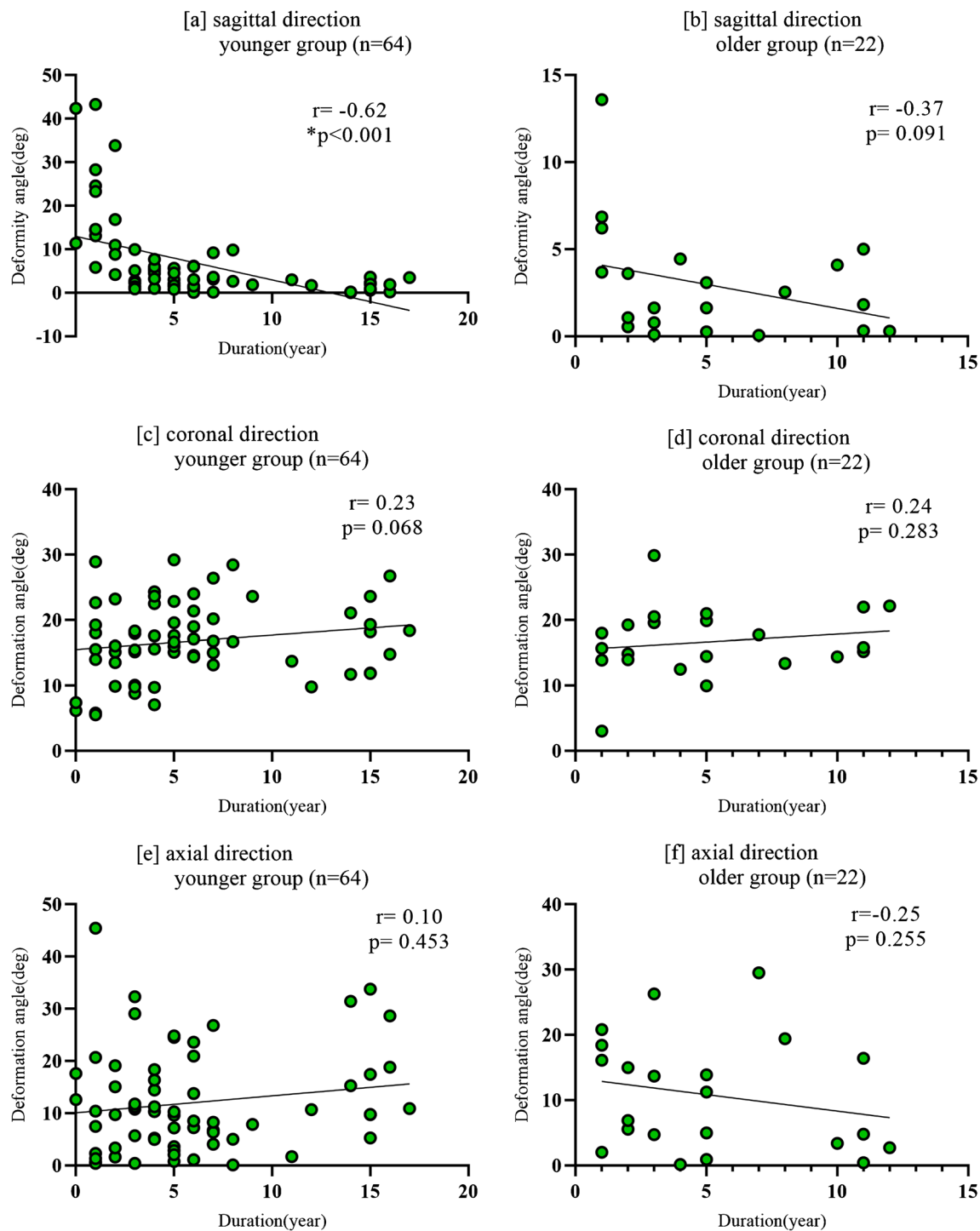
Fig. 5 The graph shows the correlation between the deformity angle and the duration with deformity at each direction in the younger group (**a**, **c**, **e**) and the older group (**b**, **d**, **f**) The correlation between the deformity angle in the sagittal direction and the duration was moderately negative in the younger group (**a**); however, no significant correlation was observed in the older group (**b**). No significant correlation was found in the coronal or axial direction between the two groups (**c–f**)

Furthermore, the insight presented herein may contribute to the determination of treatment strategies for SHFs and CVDs.

Declarations

Ethics approval The study was approved by the Institutional Review Board of Osaka University Hospital (approval number: 14179–4).

Consent to participate The requirement for written informed consent was waived because of the retrospective nature of the study.

Consent to publish This study did not include images of individual participants.

Competing interests Th authors, their immediate family, and any research foundation with which they are affiliated did not receive any financial payments or other benefits from any commercial entity related to the subject of this article.

References

1. O'Hara LJ, Barlow JW, Clarke NM (2000) Displaced supracondylar fractures of the humerus in children. Audit changes practice. J Bone Joint Surg Br 82:204–210. https://doi.org/10.1302/0301-620X.82B2.9570
2. Devnani AS (2005) Late presentation of supracondylar fracture of the humerus in children. Clin Orthop Relat Res 431:36–41. https://doi.org/10.1097/01.blo.0000152439.43810.11
3. Takeyasu Y, Murase T, Miyake J, Oka K, Arimitsu S, Moritomo H, Sugamoto K, Yoshikawa H (2011) Three-dimensional analysis of cubitus varus deformity after supracondylar fractures of the humerus. J Shoulder Elbow Surg 20:440–448. https://doi.org/10.1016/j.jse.2010.11.020
4. Smith L (1960) Deformity following supracondylar fractures of the humerus. J Bone Joint Surg Am 42-A:235–252. https://doi.org/10.2106/00004623-196547080-00021
5. Davids JR, Maguire MF, Mubarak SJ, Wenger DR (1994) Lateral condylar fracture of the humerus following posttraumatic cubitus varus. J Pediatr Orthop 14:466–470. https://doi.org/10.1097/01241398-199407000-00009
6. O'Driscoll SW, Spinner RJ, McKee MD, Kibler WB, Hastings H 2nd, Morrey BF, Kato H, Takayama S, Imatani J, Toh S, Graham HK (2001) Tardy posterolateral rotatory instability of the elbow due to cubitus varus. J Bone Joint Surg Am 83:1358–1369. https://doi.org/10.2106/00004623-200109000-00011
7. Abe M, Ishizu T, Shirai H, Okamoto M, Onomura T (1995) Tardy ulnar nerve palsy caused by cubitus varus deformity. J Hand Surg Am 20:5–9. https://doi.org/10.1016/S0363-5023(05)80047-4
8. Jeon IH, Oh CW, Kyung HS, Park IH, Kim PT (2006) Tardy ulnar nerve palsy in cubitus varus deformity associated with ulnar nerve dislocation in adults. J Shoulder Elbow Surg 15:474–478. https://doi.org/10.1016/j.jse.2005.10.009
9. Ippolito E, Moneta MR, D'Arrigo C (1990) Post-traumatic cubitus varus. Long-term follow-up of corrective supracondylar humeral osteotomy in children. J Bone Joint Surg Am 72:757–765. https://doi.org/10.2106/00004623-199072050-00017
10. Miyamura S, Oka K, Abe S, Shigi A, Tanaka H, Sugamoto K, Yoshikawa H, Murase T (2018) Altered bone density and stress distribution patterns in long-standing cubitus varus deformity and their effect during early osteoarthritis of the elbow. Osteoarthritis Cartilage 26:72–83. https://doi.org/10.1016/j.joca.2017.10.004
11. Gamble JG, Vorhies JS (2020) Remodeling of sagittal plane malunion after paediatric supracondylar humerus fractures. J Pediatr Orthop 40:e903–e909. https://doi.org/10.1097/BPO.0000000000001623
12 Attenborough CG (1953) Remodeling of the humerus after supracondylar fractures in childhood. J Bone Joint Surg Br 35-B:386–395. https://doi.org/10.1302/0301-620X.35B3.386
13. Silva M, Delfosse EM, Park H, Panchal H, Ebramzadeh E (2019) Is the "appropriate use criteria" for Type II supracondylar humerus fractures really appropriate? J Pediatr Orthop 39:1–7. https://doi.org/10.1097/BPO.0000000000001142
14. Cheng JC, Shen WY (1993) Limb fracture pattern in different paediatric age groups: a study of 3,350 children. J Orthop Trauma 7:15–22. https://doi.org/10.1097/00005131-199302000-00004
15. Persiani P, Di Domenica M, Gurzi M, Martini L, Lanzone R, Villani C (2012) Adequacy of treatment, bone remodelling, and clinical outcome in paediatric supracondylar humeral fractures. J Pediatr Orthop B 21:115–120. https://doi.org/10.1097/BPB.0b013e32834c675e
16. Bukvić N, Kvesić A, Brekalo Z, Bosak A, Bukvić F, Karlo R (2013) The problem of post-traumatic varization of the distal end of the humerus remaining after the recovery of a supracondylar fracture. J Pediatr Orthop B 22:372–375. https://doi.org/10.1097/BPB.0b013e328360f8df
17. Nikolić H, Bukvić N, Tomasić Z, Bosak A, Cicvarić T (2014) Bone remodelling after supracondylar humeral fracture in children. Coll Antropol 38:601–604
18. Simanovsky N, Lamdan R, Mosheiff R, Simanovsky N (2007) Underreduced supracondylar fracture of the humerus in children: clinical significance at skeletal maturity. J Pediatr Orthop 27:733–738. https://doi.org/10.1097/BPO.0b013e3181558a63

19. Hell AK, Gadomski C, Braunschweig L (2021) Spontaneous humeral torsion deformity correction after displaced supracondylar fractures in children. BMC Musculoskelet Disord 22:1022. https://doi.org/10.1186/s12891-021-04909-y

20. Yoon GS, Oh WT, Chun YM, Koh IH, Kang HJ, Choi YR (2020) Accuracy of conventional triplane measures compared to 3-D analysis for assessment of cubitus Varus deformities in adults. Ther Clin Risk Manag 16:349–355. https://doi.org/10.2147/TCRM.S238142

21. Pritchett JW (1988) Growth and predictions of growth in the upper extremity. J Bone Joint Surg Am 70:520–525. https://doi.org/10.2106/00004623-198870040-00007

22. Oka K, Murase T, Moritomo H, Goto A, Sugamoto K, Yoshikawa H (2009) Accuracy analysis of three-dimensional bone surface models of the forearm constructed from multidetector computed tomography data. Int J Med Robot 5:452–457. https://doi.org/10.1002/rcs.277

23. Willing RT, Lalone EA, Shannon H, Johnson JA, King GJ (2013) Validation of a finite element model of the human elbow for determining cartilage contact mechanics. J Biomech 46:1767–1771. https://doi.org/10.1016/j.jbiomech.2013.04.001

24. Wu G, van der Helm FC, Veeger HE, Makhsous M, Van Roy P, Anglin C, Nagels J, Karduna AR, McQuade K, Wang X, Werner FW, Buchholz B, International Society of Biomechanics (2005) ISB recommendation on definitions of joint coordinate systems of various joints for the reporting of human joint motion–Part II: shoulder, elbow, wrist and hand. J Biomech 38:981–992. https://doi.org/10.1016/j.jbiomech.2004.05.042

25. Kapoutsis CA, Vavoulidis CP, Pitas I (1999) Morphological iterative closest point algorithm. IEEE Trans Image Process 8:1644–1646. https://doi.org/10.1109/83.799892

26. Audette MA, Ferrie FP, Peters TM (2000) An algorithmic overview of surface registration techniques for medical imaging. Med Image Anal 4:201–217. https://doi.org/10.1016/s1361-8415(00)00014-1

27. Kim K, Yoon C, Lee HY (2023) Cubitus varus after paediatric lateral condylar fracture: true or pseudo? BMC Musculoskelet Disord 24:483. https://doi.org/10.1186/s12891-023-06604-6

28. Ga M (2015) Fractures and dislocations about the elbow. Green's skeletal trauma in children. Elsevier Saunders, Philadelphia, p 204

29. Farnsworth CL, Silva PD, Mubarak SJ (1998) Etiology of supracondylar humerus fractures. J Pediatr Orthop 18:38–42. https://doi.org/10.1097/01241398-199801000-00008

30. Celiker O, Pestilci FI, Tuzuner M (1990) Supracondylar fractures of the humerus in children: analysis of the results in 142 patients. J Orthop Trauma 4:265–269. https://doi.org/10.1097/00005131-199004030-00005

31. Jeroense KT, America T, Witbreuk MM, van der Sluijs JA (2015) Malunion of distal radius fractures in children. Acta Orthop 86:233–237. https://doi.org/10.3109/17453674.2014.981781

32. Guven MF, Kaynak G, Inan M, Caliskan G, Unlu HB, Kesmezacar H (2015) Results of displaced supracondylar humerus fractures treated with open reduction and internal fixation after a mean 22.4 years of follow-up. J Shoulder Elbow Surg 24:640–646. https://doi.org/10.1016/j.jse.2014.12.010

33. Flynn JC, Matthews JG, Benoit RL (1974) Blind pinning of displaced supracondylar fractures of the humerus in children: Sixteen years' experience with long-term follow-up. J Bone Joint Surg 56:263–272. https://doi.org/10.2106/00004623-197456020-00004

34. Worlock P (1986) Supracondylar fractures of the humerus. Assessment of cubitus varus by the Baumann angle. J Bone Joint Surg Br 68:755–757. https://doi.org/10.1302/0301-620X.68B5.3782238

35. Labelle H, Bunnell WP, Duhaime M, Poitras B (1982) Cubitus varus deformity following supracondylar fractures of the humerus in children. J Pediatr Orthop 2:539–546. https://doi.org/10.1097/01241398-198212000-00014

36. French PR (1959) Varus deformity of the elbow following supracondylar fractures of the humerus in children. Lancet 2:439–441. https://doi.org/10.1016/s0140-6736(59)90422-2

37. Kasser JR BJ (2010) Supracondylar fractures of the distal humerus. Rockwood and Wilkins' fractures in children, 7th edn. Lippincott Williams & Wilkins, Philadelphia

38. Mehlman CT, Araghi A, Roy DR (1997) Hyphenated history: the Hueter-Volkmann law. Am J Orthop (Belle Mead NJ) 26:798–800

39. Ploegmakers JJ, Verheyen CC (2006) Acceptance of angulation in the non-operative treatment of paediatric forearm fractures. J Pediatr Orthop B 15:428–432. https://doi.org/10.1097/01.bpb.0000210594.81393.fe

40. Camus T, MacLellan B, Cook PC, Leahey JL, Hyndman JC, El-Hawary R (2011) Extension type II paediatric supracondylar humerus fractures: a radiographic outcomes study of closed reduction and cast immobilization. J Pediatr Orthop 31:366–337. https://doi.org/10.1097/BPO.0b013e31821addcf